JOURNAL OF MATERIALS SCIENCE **40** (2005) 6375–6383

Transparent TiO_2 sol nanocrystallites mediated homogeneous-like photocatalytic reaction and hydrosol recycling process

YIBING XIE, CHUNWEI YUAN
Key Laboratory of Molecular & Biomolecular Electronics, Southeast University, Nanjing 210096, People's Republic of China

Published online: 18 October 2005

Lanthanide metal europium ion modified titanium dioxide (Eu^{3+}-TiO_2) sol nanocrystallites was fabricated by the wet-chemical coprecipitation-peptization method under low temperature (80°C). Eu^{3+}-TiO_2 sol particles show the anatase-rutile mixed crystal structure and the narrow particles distribution with the mean size of 6 nm. Comparing with pure TiO_2 sol, Eu^{3+}-TiO_2 sol possesses smaller primary particle size and better particulate dispersion. Transparent sol catalyst could conduct the homogeneous-like photocatalysis rather than heterogeneous one for organic pollutants degradation reaction. This crystallized Eu^{3+}-TiO_2 sol particles exhibits better interfacial adsorption effect and electron-transfer efficiency between dye molecules and catalyst particles, which contributed to stronger photocurrent response in the photoelectrochemical process. For photocatalytic degradation of azo dye, fresh Eu^{3+}-TiO_2 sol catalyst showed higher photocatalytic activity and photomineralization capability than P25 TiO_2 powder and pure TiO_2 sol under either ultraviolet light (UV) or visible light (Vis) irradiation. The recycling application of the crystallized sol catalysts was well attempted by taking advantage of its sensitivity to the medium pH value. Although Eu^{3+}-TiO_2 recycle sol had better dispersion effect and smaller secondary particles size, the absolute recovery efficiency of Eu^{3+}-TiO_2 sol particles was obvious inferior to TiO_2 sol due to its poor flocculation-separation effect. For continuous recycle use of hydrosol photocatalysis, pure TiO_2 sol demonstrates the better total discolouration efficiency than Eu^{3+}-TiO_2 sol although instinctive photochemical reactivity of fresh TiO_2 was inferior to fresh Eu^{3+}-TiO_2.

1. Introduction

Semiconductor photocatalysis has been regarded as a promising advanced oxidation technology for its degradation and mineralization of most of organic pollutants [1–3]. Semiconductor TiO_2 nanocrystallites have been extensively studied owing to its photocatalytic activity, chemical stability and nontoxicity [4]. TiO_2 phase behavior, particle stability and particle size are crucial for applications as catalysts and sensors. Generally, high temperature calcination treatment was involved to achieve phase transformation from amorphous to anatase or rutile crystal structure since amorphous TiO_2 shows its photocatalytic inactivity. However, it is still deficient to overcome the coarsening and growth of TiO_2 nanocrystallites during the high temperature heating process and serious aggregation of powder particles in aqueous slurry dispersion. It could become one of feasible solutions to fabricate crystal structure TiO_2 at mild reaction condition and conduct photodegradation reaction by sol photocatalysts [5].

Photocatalytic reaction of TiO_2 nanoparticles may be carried out either in a slurry-type system (where the catalyst particles are suspended in the aqueous solution) or in an immobilized-catalyst type system (where the catalyst particles are immobilized on the surface of various supports). The slurry-type reaction system offers significant advantages in terms of the catalyst surface availability, and superior mass-transfer properties. However, this slurry system approach requires an additional separation step to remove the catalyst from the treated water. Membrane filtration approach has been usually adopted for the nanoparticles separation from aqueous dispersion. However, nanoparticles could easily block up the micropores of the filter membrane. There are still no effective methods to regenerate the membrane for recycle use. Additionally, membrane nano-filtration is a time-consuming procedure under ambient pressure. The effective collection of nanoparticles from membrane is also one problem. Other techniques can be used but all involve nanoparticles loss, rapid deactivity and additional high expenses in a continuous photocatalytic process. This presents a major drawback to the application of such a suspension reaction system [6]. Therefore, the fine TiO_2

0022-2461
DOI: 10.1007/s10853-005-1825-y

particles are still unacceptable as an effective photocatalyst in a commercial suspension reactor due to the high costs required for separating and recovering these naoparticles from the treated water. While immobilized-catalyst type system do provide a solution to the solid-liquid separation problem, but low catalyst surface area also greatly causes its very low reaction efficiency. At present, heterogeneous photocatalysis, on a commercial scale, has still been limited to the utilization of immobilized photocatalysts although this reaction system has many weaknesses. Some research results show TiO_2 sol particles can possess a regular anatase crystal structure and such kinds of sol catalysts exhibit high photochemical reactivity, even superior to TiO_2 powder [7]. Most of all, in the field of photocatalytic degradation of organic pollutants, sol catalysts can be easily separated, collected and re-dispersed for continuous reuses by taking advantage of its sensitivity to medium pH value and electrolyte strength.

In this paper, trivalent lanthanide europium ion was selected as a dopant to improve TiO_2 catalytic property. Eu^{3+}-TiO_2 nanocrystallites were prepared under moderate reaction condition. The photocatalytic reaction was carried out in the novel hydrosol system, which could integrate the advantages of suspension and immobilization reaction system. In view of the transparent appearance of the titania sol prepared in this study, sol catalysts might behave as a homogeneous-like photocatalyst rather than a heterogeneous one. Consequently, the photocatalytic property of the transparent sol catalyst was evaluated according to degradation efficiency of organic pollutants under both UV and Vis light irradiation. Furthermore, the continuous recycling application of sol photocatalyst was investigated in hydrosol reaction system.

2. Experimental

2.1. Preparation of Eu^{3+}-TiO_2 sol nanoparticles

Eu^{3+} modified TiO_2 sol was fabricated by the wet-chemical coprecipitation-peptization method. Firstly, 50 mL precursor $TiCl_4$ was diluted and hydrolyzed with 100 mL frozen and distilled water to produce a straw yellow liquid. A proper amount of Eu_2O_3 powder was added to above solution up to 3.0% Eu^{3+} by atom fraction. This mixture was vigorously stirred till to form transparent aqueous solution. In order to ensure the complete hydrolysis reaction, a diluted $NH_3{\cdot}H_2O$ aqueous solution was added dropwise into transparent $TiCl_4$ aqueous solution till to form a white precipitate with ultimate aqueous mixture of pH 10. In order to remove these residual NH_4^+ and Cl^- ions, the precipitate was adequately washed with the deionized water and filtered with suction flask till the pH value of filtrated water was below 7.5. Then, the mixed acid of HNO_3 and HF (HNO_3/HF = 7/1, mol/mol) was used as a peptization agent to disperse the amorphous Eu^{3+}-TiO_2 sediment and the final pH value was adjusted to 1.5. The above colloid was stirred for 4 h at room temperature to form rode sol and further aged in 80°C hot water for 24 h under ultrasonic condition. Finally, Eu^{3+}-TiO_2 sol was formed with uniform, stable and transparent characteristics. The final sol can maintain uniform dispersion for quite a long time without appearing sedimentation and delamination phenomena. Pure TiO_2 sol was prepared as the same as the above process without Eu^{3+} ion addition. Eu^{3+}-TiO_2 xerogel powder was prepared from above sol products by vacuum distillation in rotary evaporator (55°C) and vacuum drying treatment in the oven (102°C).

2.2. Photoelectrochemical experiment

The photoelectrochemical property of Eu^{3+}-TiO_2 sol/X-3B was investigated under visible light irradiation. The measurements were carried out by using a standard three-electrode system equipped with a quartz window, a saturated calomel reference electrode (SCE) and a platinum plate counter-electrode (CE) placed in an undivided reaction cell. Optically transparent In_2O_3-SnO_2 oxide conductive glass (ITO) sheet was selected as working electrode. The electrolyte was Eu^{3+}-TiO_2 sol (1.0 g L^{-1}) and X-3B (100 mg L^{-1}) aqueous solution with pH 4.0. The working electrode was illuminated from the In_2O_3-SnO_2 front side. The response photocurrent-pulse time (*I–t*) measurement was recorded by using an electrochemical station (CHI660 workstation).

2.3. Photocatalytic reaction

Dyestuff compounds and intermediates have been widely used in the staining and dyeing field to cause environmental pollution. As a representative azo dye with high chemical stability, the reactive brilliant red dye X-3B (chemical formula, $C_6H_5N_2(C_{10}H_3)(OH)(NH)(SO_3Na)_2(C_3N_3)Cl_2$), was chosen as a probe compound to conduct degradation reaction. Eu^{3+}-TiO_2 and TiO_2 sol were acted as photocatalysts, Vis and UV as illuminating light source (Vis light: 150 W halogen-tungsten lamp with UV and IR cut-off filter, main wavelength 550 nm, light intensity 38.9 mW cm^{-2}; UV light: 150 W high pressure mercury lamp with water cooling jacket, main wavelength 365 nm, light intensity 6.5 mW cm^{-2}). The cold light source mainly provided visible light in the range of 400–800 nm, which was matching with the maximum absorption spectrum of X-3B (420–600 nm). The reaction mixture was vertically irradiated from the top light source and stirred at constant speed.

The photocatalytic reaction experiment was conducted in a cylindrical silica vessel. Reaction system was setup by mixing Eu^{3+}-TiO_2 or TiO_2 sol with X-3B solution. Sol photocatalyst concentration was equivalent to 1.0 g L^{-1} TiO_2 in aqueous solution. X-3B concentration was adjusted to 100 mg L^{-1} and total volume of reaction solution was 20 ml. Prior to photoreaction, the X-3B/sol mixture was magnetically stirred in dark condition for 30 min to establish the adsorption-desorption equilibrium. The analytical sample was collected every 15 min and X-3B concentration in reaction solution was determined by measuring its characteristic absorption peak intensity at 512 nm.

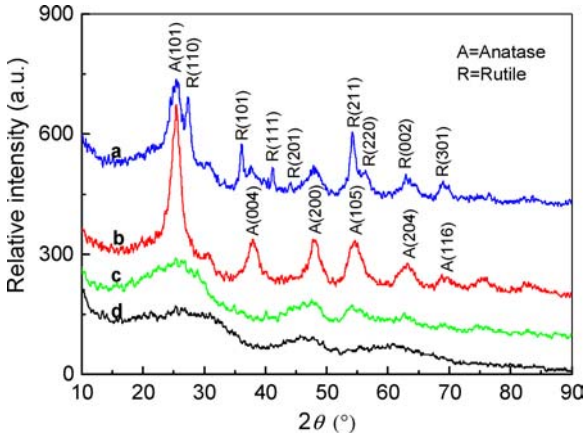

Figure 1 XRD patterns of (a) Eu^{3+}-TiO_2 sol particles with peptization-ageing treatment; (b) TiO_2 sol particles with peptization-ageing treatment; (c) Eu^{3+}-TiO_2 rude sol particles; (d) TiO_2 rude sol particles.

3. Results and discussion

3.1. Crystal structure analysis

Generally, TiO_2 sol particles usually show amorphous structure by sol-gel preparation method. Such kind of TiO_2 seldom exhibits photocatalytic activity due to non-bridging oxygen as defects in bulk TiO_2 [8]. The regular crystal structure was the prerequisite for TiO_2 acting as a photocatalyst. Additionally, different crystal phase structure also could affect physical property and photoactivity of TiO_2. Therefore, the phase behavior of sol particles was investigated by X-ray diffraction (XRD).

Although the rough diffraction peak shape had come into being at $2\theta = 25.4°$, both Eu^{3+}-TiO_2 and TiO_2 rude sol particles were still regarded as amorphous structure due to their predominant scattering peaks in XRD patterns (see Fig. 1c and d). After adequately ultrasonic peptization-ageing treatment, both Eu^{3+}-TiO_2 and TiO_2 sol particles could form anatase crystal structure due to the presence of attributive peaks ($2\theta = 25.4°$, 38.0°, 47.8°, 54.6°, 63.2°, 68.8°) (see Fig. 1a and b). It means that phase transformation from amorphous to anatase structure, which commonly requires high temperature calcination at least 415°C, could achieve during the digesting and peptizing process of rude sol at moderate operation temperature and strong acidic condition. Very broad diffraction peak at 101 crystal plane was due to its very small crystallite size of Eu^{3+}-TiO_2 sol particles. It indicates that nucleation and growth of the nanocrystallites could be affected by the doping of the lanthanide ion to bulk phase TiO_2. Additionally, XRD pattern of Eu^{3+}-TiO_2 sol also appears other diffraction peaks ($2\theta = 27.3°$, 36.1°, 41.1°, 44.0°, 54.2°, 58.3°), which was ascribed to TiO_2 rutile crystal structure (see Fig. 1a). The phase composition can be calculated using the equation of $X_A = [1 + 1.265 * (I_R/I_A)]^{-1}$, where X_R is the weight fraction of anatase in biphase composite, I_A and I_R are the intensity of anatase(101) and rutile(110) diffraction peaks respectively. X_A value was estimated at 0.7625, which means anatase TiO_2 was dominant in the mixed crystal structure. For Eu^{3+}-TiO_2 sol sample, binary phase transformation must have occurred from amorphous to the anatase-rutile crystalline structure during this peptization process. Otherwise, high temperature heating above 680°C must be provided for TiO_2 powder material to achieve the rutile phase transformation. This character is very different from single-phase-transformation of TiO_2 sol. Some research results have indicated there had existed synergistic effect between anatase and rutile nanocrystallites in the photocatalytic oxidation of organic compounds [9, 10]. Binary mixed crystal structure of Eu^{3+}-TiO_2 nanoparticles might contribute to improve its photochemical reactivity. Additionally, $Ti_{1-x}Eu_xO_2$ could be allowed to exist according to the calculation result of $0.75 < t < 1.0$ on the base of the crystal structure theory ($t = r(r_{Eu^{3+}} + r_{O^{2-}})/\sqrt{2}(r_{Ti^{4+}} + r_{O^{2-}}) = 0.7979$, $r_{Ti^{4+}} = 0.068$ nm, $r_{Eu^{3+}} = 0.0947$ nm and $r_{O^{2-}} = 0.14$ nm). Actually, Eu^{3+}-TiO_2 sol sample did not form any other new crystal diffraction peaks. The main reason was attributed to the big difference of the ionic radii between Ti^{4+} and Eu^{3+}, which would cause an inner lattice microstrain block effect. Therefore, without high temperature calcination treatment, Eu^{3+} ion would unlikely enter into the TiO_2 crystal lattice, but coordinate with dissociative oxygen anion in the surficial shallow layer to remove the oxygen defects of crystal TiO_2.

3.2. Microstructure characterization

The Eu^{3+}-TiO_2 sol morphology and particle size were investigated by transmission electron microscopy (TEM) on copper mesh by means of dip-coating preparation method and atomic force microscopy (AFM) on silica glass by means of spin-coating preparation method. TEM micrograph shows that the well-developed Eu^{3+}-TiO_2 sol particles (6 nm in mean size) dispersed uniformly in colloidal system and the continuously close-packed particles had formed an alveolate network structure. Few particle aggregations (10–20 nm in size) were ascribed to conglomeration of titania hydrate oligomer formed during peptization process (see Fig. 2a). AFM micrograph shows that Eu^{3+}-TiO_2 sol particles had a spheroidal shape and distributed homogenously on the support. The average size was about 8 nm (see Fig. 2b). So, the measured particle size of Eu^{3+}-TiO_2 sol sample was in agreement with each other by using AFM and TEM method. The above result also means that Eu^{3+} ion modification preferably retarded aggregation and growth of well-dispersed sol particles, which resulted in the decrease of TiO_2 particle size.

3.3. Spectrum absorption

The UV-Vis absorption spectra of different colloidal solutions are illustrated in Fig. 3. All above catalysts are adjusted to the same concentration in aqueous solution for spectrum measurement. It can be seen that both Eu^{3+}-TiO_2 and pure TiO_2 did not show any spectrum absorption in visible range (wavelength $\lambda > 400$ nm). The only strong absorption in the ultraviolet range was owe to the change-transfer process from 2p orbital of O^{2-} ions to t_{2g} orbital of the Ti^{4+} ions in the bulk TiO_2 oxide. It means both sol catalysts cannot drive the direct

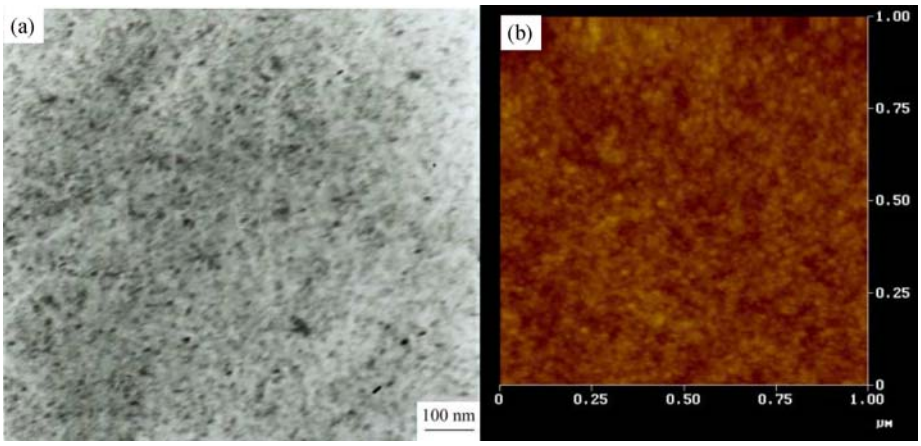

Figure 2 (a) TEM and (b) AFM micrograph of Eu^{3+}-TiO_2 sol particles.

photocatalysis under visible light irradiation. Moreover, the spectrum absorption band-edge appeared obvious blue-shift, which was ascribed to the quantum size effect of sol nanoparticles. The optical absorption onset was estimated at 330 nm for Eu^{3+}-TiO_2 sol and 345 nm for TiO_2. The corresponding band-gap energy was identified as 3.76 eV for Eu^{3+}-TiO_2 and 3.60 eV for TiO_2 nanocrystallites. This blue-shift is relative to quantum dot of the synthesized ultrafine nanocrystals in hydrosol solution. Additionally, UV spectrum absorption intensity of Eu^{3+}-TiO_2 was stronger than pure TiO_2. Therefore, sol particle size affects optical properties of their dispersions. The increase in optical absorption of UV radiation was associated with the improvement of sol particles dispersion and the reduction of particle size. Previous experimental results by AFM measurement also showed that the average size of Eu^{3+}-TiO_2 sol particles (c.a. 8 nm) was smaller than that of pure TiO_2 sol particles (c.a. 20 nm). So, the spectrum experiment results were good agreement with the AFM observation results. Furthermore, both Eu^{3+}-TiO_2 and TiO_2 sol particles possessed much smaller mean size than P25 TiO_2 slurry particle (40 nm). The decrease of colloid particle size in sol could promote the light radiation absorption, which might eventually improve the photon-transfer efficiency during the photochemical reaction.

3.4. Interfacial adsorption effect

Surface properties play an important role in photocatalytic reaction since this process usually occurs at the interface between catalyst particles and reaction substrates [11]. This role essentially increases in the case of nanocrystalline quantum dot materials due to their large surface-to-volume ratio. The adsorption behavior was investigated between azo dye X-3B and Eu^{3+}-TiO_2 sol photocatalyst. The aqueous mixture of Eu^{3+}-TiO_2 sol and X-3B was adequately stirred in the dark condition. The adsorption-desorption equilibrium was almost established after 30 min since UV-Vis absorption spectrum of X-3B in bulk solution almost had no change. Thus, X-3B concentration in this mixture system was measured during the whole physical adsorption process and the experimental results were shown in Fig. 4.

In X-3B/sol catalyst mixture system, X-3B concentration was constant at 100 g L^{-1} and sol catalyst concentration was increased from 0 to 2.0 g L^{-1}. During this process, X-3B characteristic absorption peak intensity at 512 nm obviously declined after adequate interfacial adsorption. It means that X-3B molecules adsorbed by Eu^{3+}-TiO_2 sol particles gradually rose with the increase of sol concentration. Saturation adsorption concentration of sol photocatalysts was about

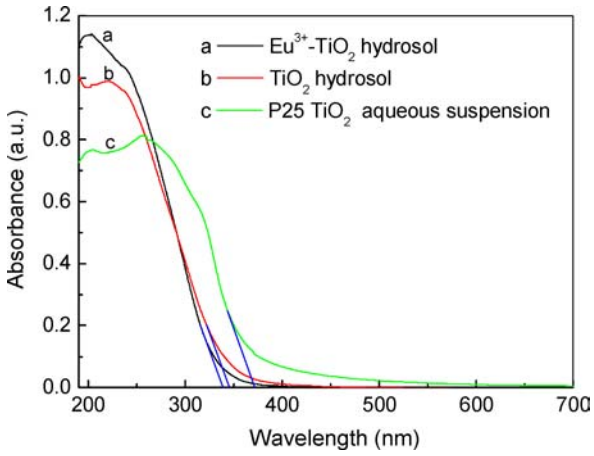

Figure 3 UV-Vis absorption spectra of (a) Eu^{3+}-TiO_2 hydrosol, (b) TiO_2 hydrosol and (c) P25 TiO_2 powder suspension.

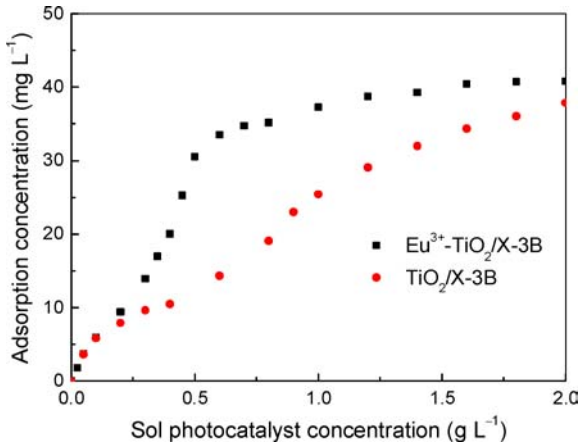

Figure 4 Adsorption concentration of X-3B(c_a) in terms of sol photocatalyst concentration (c_p) (X-3B/Eu^{3+}-TiO_2 adsorption curve fitting formula: $c_a = 43.53 * [1-\exp(-1.804c_p)]$, correlation coefficient $R = 0.9849$; X-3B/TiO_2 adsorption curve fitting formula: $c_a = 55.71 * [1 - \exp(-0.5857c_p)]$, correlation coefficient $R = 0.9937$).

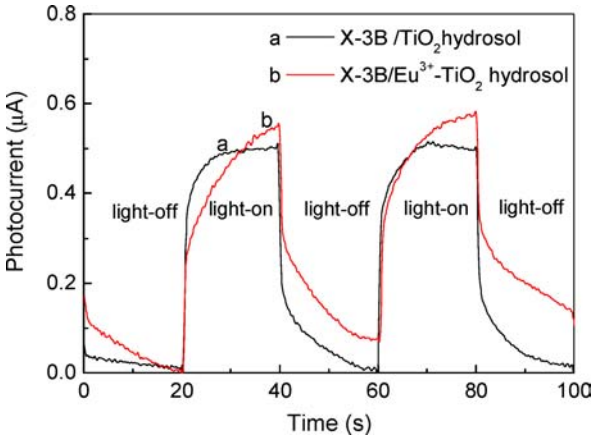

Figure 5 Photocurrent response of ITO electrode in (a) X-3B/TiO_2 and (b) X-3B/TiO_2 hydrosol system under visible light/dark pulse irradiation condition.

0.6 g L^{-1} for Eu^{3+}-TiO_2 and 1.0 g L^{-1} for TiO_2. Therefore, Eu^{3+}-TiO_2 hydrosol system exhibited the more effective interfacial adsorption to organic molecule than pure TiO_2. The affinity property between substrates and photocatalysts was a key driving factor to affect overall degradation reaction rate [12]. Regarding the strong adsorption property of X-3B on the surface of Eu^{3+}-TiO_2 nanoparticles, the main reason was the electrostatic action force between the positive charge of Eu^{3+} modification ion of TiO_2 and the negative charge of anionic dye X-3B with $–SO_3Na$ functional groups. Eu^{3+}-TiO_2 shows its capability to form chemical complexes of $R—SO_3^-\cdots Eu^{3+}$-TiO_2, which could enhance the interface adsorption in aqueous solution. Another important factor was attributed to the well dispersed ultrafine sol particles with a very weak natural aggregation property in aqueous solution. It can provide high interfacial reaction areas. Thus, incorporation of europium ion into TiO_2 matrix could provide an effective method to concentrate the organic pollutant on the surface of catalyst particles.

3.5. Photoelectrochemical property

The photocatalytic activity of TiO_2 nanocrystallites depends on the overall efficiency of electron generation, charge transfer and separation [13, 14]. In order to investigate the interfacial electron-transfer process between Eu^{3+}-TiO_2 (or TiO_2) particles and probe molecules, photoelectrochemical experiment was especially designed and the response photocurrent was also carried out under visible light illumination. This experimental condition was kept the same as that in photocatalysis so as to simulate the same working condition in dye/Eu^{3+}-TiO_2 bulk aqueous solution. The response photocurrent-pulse time profiles without applying any bias electrode potential were illustrated in Fig. 5.

For X-3B/TiO_2 hydrosol system, photocurrent rapidly generated at the beginning of visible light illumination, and simultaneously increased to a steady value of 0.495 μA within a short time. Once light-off, photocurrent intensity rapidly dropped down to initial value of 0 μA. The photocurrent response had no decay in intensity and no downward/upward peak under the light-on condition because of fast transfer of the photogenerated electrons through out-circuit. The photocurrent intensity was stable at interval of 20 s under visible light irradiation. For X-3B/Eu^{3+}-TiO_2 hydrosol system, when light-on, the photocurrent instantly generated, then gradually increased to peak value of 0.565 μA as its photocurrent. Once light-off, it drastically fell down, then decreased to 0.087 μA as its dark current. For photoelectrochemical experiment of Eu^{3+}-TiO_2/X-3B, photocurrent response appeared an apparent delay phenomenon under visible light pulse irradiation.

Eu^{3+}-TiO_2 and TiO_2 hydrosol in X-3B solution shows the different photocurrent response. Electron-transfer effect plays an important role between sol particles and probe molecules [15]. Regarding the three phase action interface of Dye—Eu^{3+}-TiO_2 (or TiO_2)—ITO, electrons was generated from the excitation-state dye molecule and then injected into TiO_2 conduction-band. Some of the accumulation electrons in TiO_2 conduction band could subsequently transfer to ITO electrode to form out-current. Considering difference of the excitation photocurrent intensity, excitation electrons injection could be more effective between X-3B molecule and Eu^{3+}-TiO_2 sol particles. In this case, Eu^{3+} ion could act as Lewis acid because of their partial unoccupied 4f atomic orbits while azo dye could act as Lewis base due to its big π electron conjugation structure. Lewis acid-base complex between europium ion and azo dye could form a feasible electron-transfer channel. Thus, interaction effect of Eu^{3+}-TiO_2 was superior to pure TiO_2 sol. The electron-transfer route in Dye $\rightarrow$ Eu^{3+}-TiO_2 $\rightarrow$ ITO was more effective than that in Dye $\rightarrow$ TiO_2 $\rightarrow$ ITO. On the other hand, modification ion Eu^{3+} could also act as a good electron-scavenger to trap conduction band electrons since the standard redox potential of Eu^{3+}/Eu^{2+} (-0.35 V vs. NHE) was more positive than TiO_2 conduction band potential (-0.5 V vs. NHE). This factor partly restrained the free transfer of out-current electrons in Eu^{3+}-TiO_2 system. Therefore, in the photocurrent response, photocurrent intensity had emerged an apparent delay phenomenon under visible light/dark pulse irradiation condition.

3.6. Photocatalytic activity

Photocatalytic activity of sol particles was assessed by investigating photodegradation efficiency of X-3B in hydrosol reaction system. UV-Vis absorption spectra of X-3B reaction products were measured every 15 min interval when Eu^{3+}-TiO_2 (or TiO_2) sol photocatalysis was induced by visible light or UV light. Sol catalyst concentration was 1.0 g L^{-1}. The original X-3B concentration was 100 mg L^{-1} and its total organic carbon (TOC) value was 15.6 mg L^{-1}. P25 TiO_2 powder, as a standard catalyst, was also used in the photoreaction experiments in order to compare the photoactivity with sol catalyst. Additionally, the reaction products after 120 min photocatalysis were collected for X-3B concentration and TOC value measurement in order

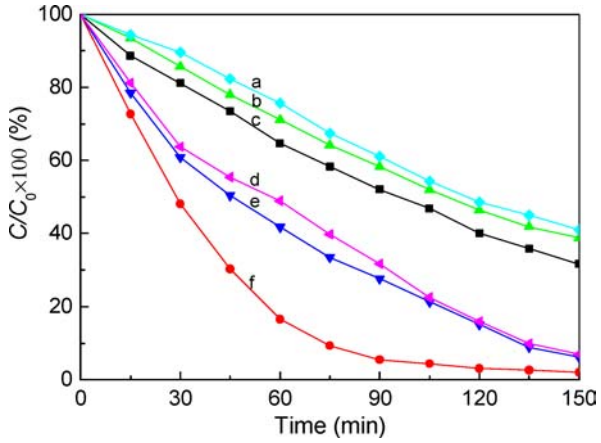

Figure 6 X-3B degradation effect in terms of reaction time in (a) Vis+P25 TiO_2 powder (b) Vis+TiO_2 sol+X-3B; (c) Vis+Eu^{3+}-TiO_2 sol+X-3B; (d) UV+P25 TiO_2 powder+X-3B; (e) UV+TiO_2 sol+X-3B; (f) UV+Eu^{3+}-TiO_2 sol+X-3B reaction system (C_0 (TiO_2 sol + X-3B) = 67.57 mg L^{-1}), C_0 (Nd^{3+}-TiO_2 sol + X-3B) = 63.66 mg L^{-1}, C_0 (P25 TiO_2 powder + X-3B) = 84.70 mg L^{-1}).

to compare the degradation and mineralization degree in different reaction system. Experimental results were summarized in Fig. 6 and Table I.

In view of dark adsorption, X-3B concentration in bulk solution decreased from 100 to 84.70 mg L^{-1} for P25 TiO_2 suspension system, 63.66 mg L^{-1} for TiO_2 hydrosol system and 67.57 mg L^{-1} for Eu^{3+}-TiO_2 hydrosol system, respectively. It means that Eu^{3+}-TiO_2 sol particles showed more effective interfacial adsorption capability than TiO_2 sol and P25 TiO_2 powder particles. Moreover, both Eu^{3+}-TiO_2 and pure TiO_2 sol catalysts demonstrated higher photodegradation efficiency than P25 TiO_2 powder under either UV or Vis light excitation. It indicates that transparent sol catalyst could favor the light-transfer and mass-transfer. The homogeneous-like reaction in transparent hydrosol system could be more effective than the heterogeneous one in powder suspension system. The linear fit relationship between $\ln(C_0/C)$ and reaction time t could also be observed for hydrosol reaction system. X-3B dye degradation reaction followed a pseudo-first-order kinetic characteristic and degradation rate curves could be described using Langmuir-Hinshelwood formula. The corresponding apparent reaction rate constants were observed to obey the following order of UV/Eu^{3+}-TiO_2 (0.02773) > UV/TiO_2 (0.01554) > Vis/Eu^{3+}-TiO_2 (0.00749) > Vis/TiO_2 (0.00673). Regarding photomineralization effect, the same order was observed for the total TOC removal ratio. Accordingly,

TABLE I X-3B degradation and mineralization effects in hydrosol and suspension reaction system after 120 min photocatalysis

Reaction system	Half-life time (min)	Degradation ratio (%)	Mineralization ratio (%)
(Vis+P25 TiO_2)	115.8	51.4	10.7
(Vis+TiO_2)	103.1	53.6	11.3
(Vis+Eu^{3+}-TiO_2)	92.5	60.1	40.4
(UV+P25 TiO_2)	57.3	84.1	62.6
(UV+TiO_2)	44.6	84.9	59.8
(UV+Eu^{3+}-TiO_2)	25.0	96.4	79.3

photodegradation and photomineralization capability of Eu^{3+}-TiO_2 sol catalyst under UV light was apparently superior to that under visible light irradiation. Using UV light resulted in a better photodegradation performance than using visible light for Eu^{3+}-TiO_2 or TiO_2. Meanwhile, lanthanide Eu^{3+} ion modification to TiO_2 could obviously promote photocatalytic activity of sol nanoparticles.

Different reaction mechanism caused these differences. The bulk band-gap of anatase crystal TiO_2 was 3.2 eV, which can only be excited by UV light ($\lambda < 387$ nm). Excitation energy of X-3B dye molecule was 2.36 eV, which was responded to visible light. Therefore, UV/X-3B/Eu^{3+}-TiO_2 hydrosol system mainly underwent direct photocatalysis reaction although indirect sensitization reaction mechanism also coexisted. However, Vis/X-3B/Eu^{3+}-TiO_2 hydrosol system only underwent sensitized-photocatalysis reaction [16]. Direct UV/photocatalysis process involved the charge separation in one step ($TiO_2 + UV \rightarrow TiO_2(CB)\cdots e^- + TiO_2(VB)\cdots h^+$). It was a homogeneous process to achieve electron-transition from valance band to conduction band of TiO_2 nanocrystallites within a single step. Vis/sensitized-photocatalysis underwent the charges separation in two steps. Step1: Electrons of dye molecule were transited from ground state to excitation state by absorption visible light photons (dye + Vis $\rightarrow$ dye* $\rightarrow$ $[dye^{+\cdot}\cdots e^-]^*$). Step2: Electrons were successively transferred from dye* to TiO_2(CB) through heterogeneity injection process ($[dye^{+\cdot}\cdots e^-]^* + TiO_2(CB) \rightarrow TiO_2(CB)\cdots e^- + dye^{+\cdot}$) Electron-transfer process was achieved in a single-step under UV light irradiation. However, such a process needed two steps to accomplish under visible light irradiation. As an overall rate determining step, a limited heterogeneous electrons-transfer from dye$*$ to TiO_2(CB) would inhibit the charge separation efficiency of $[dye^{+\cdot}\cdots e^-]$. Actually, UV/photocatalysis mainly contributed mineralization effect while Vis/sensitized-photocatalysis mainly exhibited the selective oxidation effect. Additional, each crystal could act as a nanoreactor. As the consequence of quantum dot effect and special surface area, both photons absorption and substrates adsorption could associate with the photochemical reactivity of sol catalyst. These factors jointly caused the difference in X-3B photocatalytic degradation efficiency under both UV and visible light excitation.

3.7. Sol photocatalyst recycling application

The regeneration and recycle use of catalysts were one of key steps to realize photocatalysis technology for practical applications [17]. Particularly, the recycling application of sol catalyst was designed and continuous photocatalytic reaction was carried out by using the same sol particles. Sol catalyst was sensitized to pH value and electrolyte strength in aqueous medium. They could flocculate and delaminate when the pH value was adjusted to certain alkaline range. The obtained flocculation products can be re-dispersed into sol system by forcibly ultrasonic treatment under certain acidic

TABLE II Residual X-3B and sol catalyst concentration in supernatant after 120 min photocatalysis in X-3B/TiO_2 (Eu^{3+}-TiO_2) hydrosol recycling reaction system

Recycling times of sol photocatalyst	1 sol	2 sol	3 sol	4 sol	5 sol
X-3B concentration after TiO_2 catalysis	1.68	7.32	10.62	13.66	22.50
TiO_2 concentration after recycle use	0.074	0.049	0.045	0.036	0.024
X-3B concentration after Eu^{3+}-TiO_2 catalysis	4.28	11.88	22.36	39.25	51.36
Eu^{3+}-TiO_2 concentration after recycle use	0.117	0.076	0.063	0.052	0.044

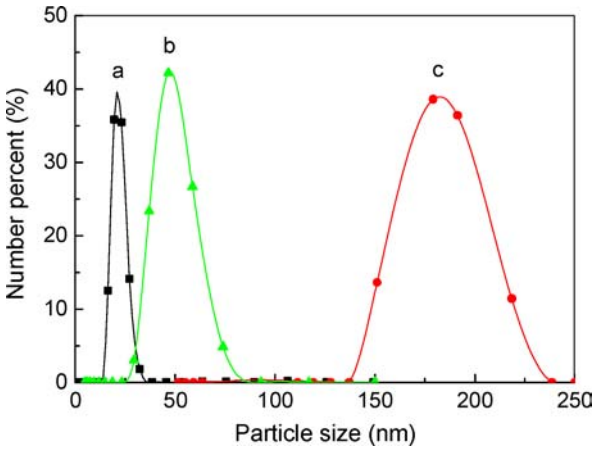

Figure 7 PSD of (a) new prepared fresh TiO_2 sol, (b) TiO_2 sol after one time recycling photocatalysis and (c) TiO_2 sol after five times recycling photocatalysis.

condition. According to this property of sol catalyst, the recycling photocatalysis was designed under visible light irradiation in order to examine the feasibility of Eu^{3+}-TiO_2 sol for continuous reuse. Firstly, reaction product of 20 mL Vis/X-3B/Eu^{3+}-TiO_2 hydrosol was collected after 120 min photocatalysis. The pH value of mixture solution was adjusted to 9.0–10 with $NH_3 \cdot H_2O$ solution. Transparent supernatant could be removed by physical separation method after the whole colloid was settled for 60 min. The collected flocculation could be dispersed into translucent secondary Eu^{3+}-TiO_2 hydrosol by means of ultrasonic dispersion along with adequately stirring while its pH value was adjusted to 2.0 with nitric acid solution. Then, the recovery Eu^{3+}-TiO_2 sol was applied to prepare total 20 mL hydrosol reaction system (pH = 4.0) with X-3B (ultimate concentration 100 mg L^{-1}) for next round photocatalysis. Finally, after flocculation separation of X-3B/sol catalyst mixture, X-3B concentration was directly determined by UV-Vis absorption spectrum method and catalyst concentration was measured by thermogravimetric analysis method in supernatant. The above process was repeated to realize the recycling application of sol photocatalyst. The same operation process was adopted for X-3B/TiO_2 hydrosol system. The whole experimental process included both photochemical degradation and flocculation-separation which jointly contributed the total discolouration of azo dye. Experimental results of recycling application of sol catalyst were summarized in Table II.

Initial X-3B concentration, 100 mg L^{-1}; initial concentration of new fresh sol catalyst, 1.0 g L^{-1}; total volume of X-3B/sol catalyst, 20 mL; 1 sol, 2 sol, 3 sol, 4 sol and 5 sol representing the reusing times of the same sol catalyst.

Table II shows that X-3B concentration in supernatant was very low during TiO_2 sol recycling photocatalysis and X-3B removal ratio still kept above 90% after 3 times reuse. Even after 5 times reuse, total discolouration efficiency was above 77% by TiO_2 recycle sol. It means that TiO_2 sol could act as a useful photocatalyst to drive continuous photodegradation reaction. Most importantly, TiO_2 sol could be reused for several times without a rapid decline of dye removal efficiency. With respect to the hydrosol recycling photocatalysis, Eu^{3+}-TiO_2 recycle sol could keep high photochemical reactivity. Total dye removal ratios were 95.72% and 88.12% respectively during the first two recycle uses. Comparatively, the total discolouration efficiency had obviously descended to below 50% after five times of recycling photocatalysis by Eu^{3+}-TiO_2 recycle sol. So, although fresh Eu^{3+}-TiO_2 sol revealed very high photocatalytic degeadation efficiency, its photochemical reactivity sharply declined during continuous recycling photocatalysis. Regarding the sol catalyst in supernatant, the concentration of either TiO_2 or Eu^{3+}-TiO_2 gradually decreased with increasing the recycling times. Furthermore, the recovery amount of TiO_2 sol catalyst was higher than Eu^{3+}-TiO_2 for each reuse. It means that the smaller sol particles caused the lower recovery efficiency by flocculation-separation process. The instinctive catalytic activity, as well as the recovery efficiency of sol catalyst, affected the photodegradation reaction during the recycling application. In current situation, the absolute catalyst amount became the predominant affecting factor. These experimental results could well explain the reason why Eu^{3+}-TiO_2 sol exhibited the lower decolouration effeciency than TiO_2 sol during the continuous recycling photocatalysis.

The sol particles in the whole dispersion system seldom keep the same size during the recycling photocatalytic process. Their size may change and distribute over a certain range. The particle size distribution (PSD) of counting number percent was measured in aqueous solution by light scattering particle zetasizer.

Fig. 7 shows both fresh TiO_2 sol and recycle sol particles had single-modal distribution characteristic. The particle size distribution was from 14 to 35 nm with the maximum peak at 21 nm for new prepared fresh TiO_2 sol, from 24 to 92 nm with the maximum peak at 47 nm for one time recycle sol and from 137 to 239 nm with the maximum peak at 182 nm for five times recycle sol. Fresh TiO_2 sol particles displayed narrow distribution with small particle size. Comparatively, the reused TiO_2 sol particles size gradually increased and its distribution became broader during the continuous recycling application.

Similar PSD experimental result was obtained for Eu^{3+}-TiO_2 sol. Both fresh Eu^{3+}-TiO_2 sol and recycle

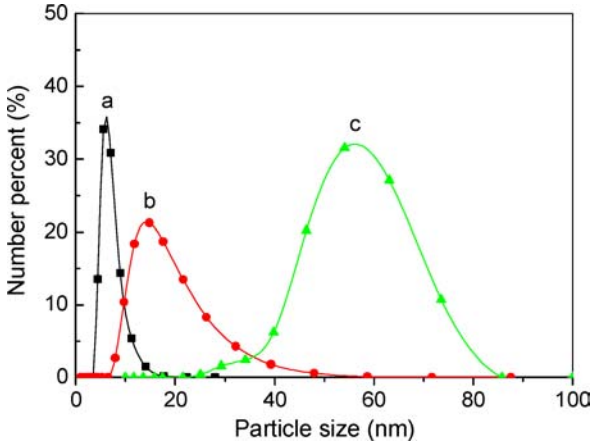

Figure 8 PSD of (a) new prepared fresh Eu^{3+}-TiO_2 sol, (b) Eu^{3+}-TiO_2 sol after one time recycling photocatalysis and (c) Eu^{3+}-TiO_2 sol after five times recycling photocatalysis.

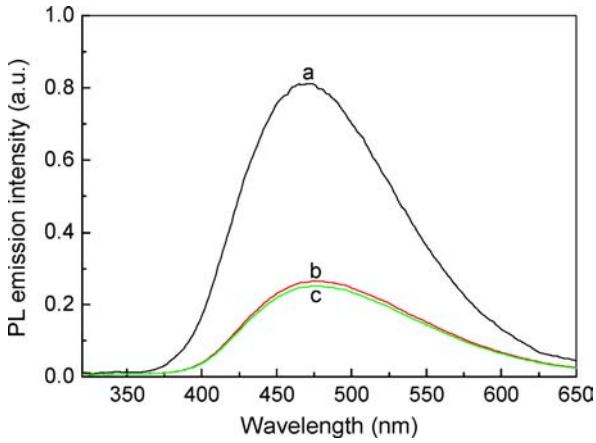

Figure 9 PL emission spectra of (a) TiO_2 (b) Eu^{3+}-TiO_2 after recycling five times and (c) fresh Eu^{3+}-TiO_2 hydrosol by using 325 nm as an excitation wavelength.

sol particles also had single-modal distribution characteristic. The particle size distribution was from 3 to 17 nm with the maximum peak at 6 nm for fresh Eu^{3+}-TiO_2 sol, from 6 to 58 nm with the maximum peak at 21 nm for one time recycle sol and from 24 to 86 nm with the maximum peak at 56 nm for five times recycle sol. The fresh Eu^{3+}-TiO_2 sol particles displayed very narrow distribution with small particle size. However, along with continuous recycle use, both distribution range and its mean size gradually increased for Eu^{3+}-TiO_2 sol particles (see Fig. 8).

Obviously, primary particles cluster (identified as ~6 nm for Eu^{3+}-TiO_2 and ~21 nm for TiO_2 by PSD) could stand together to form the secondary particles (~21 nm and ~47 nm respectively) by means of physical attractive forces. On the one hand, TiO_2 agglomerates from the secondary particles were robust and not easily broken down into their primary constituents, which restrict the subsequent dispersion in liquids. On the other hand, this property facilitated the separation of TiO_2 nanoparticles during recycling process. Comparatively, it became disadvantageous for Eu^{3+}-TiO_2 nanoparticles recovery by the flocculation-separation process due to the less aggregation effect in the dispersion solution. The inherent reactivity of fresh hydrosol and the secondary dispersion colloid of recycle sol differentiate their discolouration efficiency in the dye degradation reaction. In general, after continuous recycle use, the average particle size definitely increased and particles distribution range surely broadened for recycle sol nanoparticles on the behalf of individual particles hard aggregation and poor dispersion effects. Meanwhile, the absolute recovery amount of sol particles also declined due to incomplete particles separation. As a result, reaction efficiency of recycle sol photocatalysts must be descending gradually except in the respect of the declining degree.

Photoluminescence (PL) techniques have been widely used to investigate the structure and property of the active sites on the surface of metal oxides semiconductors because of its high sensitivity and nondestructive character [18]. To better understand the possible leaching loss of Eu^{3+} ions during the recycling photocatalysis of Eu^{3+}-TiO_2 nanoparticles, PL emission spectrum of Eu^{3+}-TiO_2 were examined during the hydrosol recycling catalysis.

Fig. 9 shows that PL main peak of TiO_2 occurred at 468 nm while Eu^{3+}-TiO_2 located at 474 nm, which originated from the charge-transfer transition from TiO_2 donor levels to the valence band at the sites near defects. Additionally, PL intensity of TiO_2 was significantly higher than that of Eu^{3+}-TiO_2. PL peak position of TiO_2 shifted to red direction with modification by 3.0 atom% europium ion. If we agree that the PL emission mainly results from the recombination of the excited free carriers, the lower PL intensity indicates a lower radiative recombination of electron-hole pairs. Considering PL emission spectrum of Eu^{3+}-TiO_2, its lower intensity may imply the fact that electron-transfer must have occurred from donor levels of host (TiO_2) to the crystal field states of guest (Eu^{3+}). Furthermore, PL peak intensity of the recycled Eu^{3+}-TiO_2 shows a little increase in comparison with fresh Eu^{3+}-TiO_2. But the increase degree was less than 3.4%. It indicates that Eu^{3+}-TiO_2 sol catalyst exhibited a certain chemical stability and the leaching loss of Eu^{3+} was negligible during the recycling photocatalysis. Eu^{3+} ions could not replace Ti^{4+} in anatase crystal lattice but well coordinate with O^{2-} during chemical peptization process to form defect-states oxide on the surficial shallow layer of crystal TiO_2. Accordingly, the decline of total discolouration efficiency of Eu^{3+}-TiO_2 sol was unlikely caused by the leaching loss of Eu^{3+} during the hydrosol recycling catalysis.

For sol recycling photocatalysis, total discolouration effect of dye was ascribed to the synergistic result of chemical photocatalysis decomposition and physical flocculation separation in hydrosol recycling reaction system. The instinctual photoactivity, recovery amount and dispersion effect of sol photocatalysts would contribute together to affect the photocatalytic decomposition efficiency. However, it was completely opposite physical process for hydrosol system between particles dispersion and flocculation [19]. Eu^{3+}-TiO_2 sol has smaller particle size and better dispersion effects than TiO_2 sol, but the flocculation-separation process

more difficult during the recycling application. Although Eu^{3+}-TiO_2 sol catalyst has very high instinctive photochemical reactivity, the recovery amount of Eu^{3+}-TiO_2 sol catalyst was less than that of TiO_2 sol during each recycle. Eu^{3+}-TiO_2 sol showed lower removal ratio of X-3B than TiO_2 sol after continuous recycling photocatalysis. Therefore, both TiO_2 and Eu^{3+}-TiO_2 sol catalyst have their respective advantages and both of them could act as a useful photocatalyst to drive photochemical reaction. Sol nanoparticles, as a novel catalyst, feasible to be recovered for continuous recycling photocatalytic reaction, exhibits potential application although it still needs to improve reusing times meanwhile keeping high photoactivity.

4. Conclusions

The composite nanocrystallites Eu^{3+}-TiO_2 was prepared in moderate reaction temperature and ambient pressure. Lanthanide europium ion modification could obviously improve sol particles dispersion and interfacial adsorption effects, which promoted the photocatalytic activity for azo dye degradation. Homogeneous-like reaction system conducted by transparent crystallized sol catalyst was much effective than heterogeneous reaction in powder suspension system. Dye/UV/sol system showed better photodegradation and photomineralization effect by direct photocatalysis than Dye/Vis/sol system by the sensitized-photocatalysis. Moreover, fresh Eu^{3+}-TiO_2 sol exhibited higher activity for X-3B degradation than pure TiO_2 sol and P25 TiO_2 powder catalyst. The difference of photoreactivity was fundamentally ascribed to the factors of electrons excitation, transfer and separation efficiency in different reaction systems. For continuous recycling process of hydrosol photocatalysis, pure TiO_2 sol has shown better discolouration effect than Eu^{3+}-TiO_2 mainly due to its more effective flocculation-separation and higher recovery of pure TiO_2 sol nanoparticles.

Acknowledgements

This work was financially supported by the Hi-Tech Research and Development? Program (863 Program) of China (No. 2002AA302304) and the National Natural Science Foundation of China (No. 60121101).

References

1. R. ANDREOZZI, V. CAPRIO, A. INSOLA and R. MAROTTA, *Catal. Today* **53** (1999) 51.
2. M. PEREZ, F. TORRADES, X. DOMENECH and J. PERAL, *J. Chem. Technol. Biotechnol.* **77** (2002) 525.
3. E. BRILLAS, E. MUR, R. SAULEDA, L. SANCHEZ, J. PERAL, X. DOMENECH and J. CASADO, *Appl. Catal. B: Environ.* **16** (1998) 31.
4. A. FUJISHIMA, T. N. RAO and D. A. TRYK, *J. Photochem. Photobiol. C: Photochem. Rev.* **1** (2000) 1.
5. S. S. WATSON, D. BEYDOUN, J. A. SCOTT and R. AMAL, *Chem. Eng. J.* **95** (2003) 213.
6. P. FERNÁNDEZ-IBÁÑEZ, J. BLANCO, S. MALATO and F. J. DELAS NIEVES, *Water Res.* **37** (2003) 3180.
7. E. GHENNE, F. DUMONT and C. BUESS-HERMAN, *Colloid Surf. A* **131** (1998) 63.
8. P. P. AHONEN, O. RICHARD and E. I. KAUPPINEN, *Mater. Res. Bull.* **36** (2001) 2017.
9. T. OHNO, K. TOKIEDA, S. HIGASHIDA and M. MATSUMURA, *Appl. Catal. A: General* **244** (2003) 383.
10. C. WU, Y. YUE, X. DENG, W. HUA and Z. GAO, *Catal. Today* **93–95** (2004) 863.
11. S. HORIKOSHI, H. HIDAKA and N. SERPONE, *J. Photochem. Photobiol. A: Chem.* **138** (2001) 69.
12. M. BOWKER, D. JAMES, P. STONE, R. BENNETT, N. PERKINS, L. MILLARD, J. GREAVES and A. DICKINSON, *J. Catal.* **217** (2003) 427.
13. E. GALOPPINI and W. GUO, *J. Am. Chem. Soc.* **123** (2001) 4342.
14. S. HORIKOSHI, N. SERPONE, J. ZHAO and H. HIDAKA, *J. Photochem. Photobiol. A: Chem.* **118** (1998) 123.
15. G. BURGETH and H. KISCH, *Coordin. Chem. Rev.* **230** (2002) 40.
16. T. BAN, S. KONDOH, T. OHYA, Y. OHYA and Y. TAKAHASHI, *J. Photochem. Photobiol. A: Chem.* **156** (2003) 219.
17. D. BEYDOUN, R. AMAL, J. SCOTT, G. LOW and S. MCEVOY, *Chem. Eng. Technol.* **24** (2001) 745.
18. K. FUJIHARA, S. IZUMI, T. OHNO and M. MATSUMURA, *J. Photochem. Photobiol. A: Chem.* **132** (2000) 99.
19. P. JENKINS and M. SNOWDEN, *Adv. Colloid Interface Sci.* **68** (1996) 57.

Received 26 February
and accepted 2 May 2005